

SHORT-TERM TENSILE STRENGTH OF CFRP LAMINATES FOR FLEXURAL STRENGTHENING OF CONCRETE GIRDERS

Ayman M. Okeil

Visiting Assistant Professor, Dept. of Civil and Env. Engineering, University of Central Florida, Orlando, FL 32816-2450, Tel.: (407) 823-3779, Fax: (407) 823-3315, aokeil@maha.engr.ucf.edu

Sherif El-Tawil

Assistant Professor, Dept. of Civil and Env. Engineering, University of Central Florida, Orlando, FL 32816-2450

Mohsen Shahawy

Chief Structural Analyst, Structural Research Center, Florida Department of Transportation, 2007 East Dirac Drive, Tallahassee, FL 32310.

ABSTRACT

Externally bonded carbon fiber reinforced polymer (CFRP) laminates are proven to be a feasible alternative to traditional methods for strengthening and stiffening deficient reinforced concrete and prestressed concrete girders. However, there is a general lack of established techniques for estimating a reliable value for the short-term tensile strength of the CFRP laminates. Manufacturers typically list the strength of an individual fiber or dry strand in the product data sheet and not that of the laminate, leaving engineers no choice but to resort to coupon tests. A method based on the Weibull theory for brittle material is presented to estimate the strength of unidirectional CFRP laminates using the statistical properties of the constituent fibers. The methodology accounts for the size effect and the existence of stress gradients. Good agreement is found between theory and experimental results. The design implications of the developed methodology are discussed, and a chart is provided for quantifying the size effect.

KEYWORDS

bridges (structures), beams (girders), size effect, Weibull Theory, tensile strength, CFRP.

RESEARCH SIGNIFICANCE

Obtaining a reliable estimate of the short-term tensile strength of CFRP laminates is essential for design and analysis of concrete girders rehabilitated with CFRP material. This research presents a method for estimating the strength of CFRP laminates based on the Weibull Theory. The developed method is verified by comparing to test data and is used to develop a design chart, which can be utilized in the design of beams strengthened with CFRP laminates.

INTRODUCTION

Extensive research has shown that externally bonded carbon fiber reinforced polymer (CFRP) material in the form of plates or laminates is particularly suited for flexural strengthening and stiffening of deficient reinforced concrete (RC) and prestressed concrete (PC) girders. Concrete beams may be flexurally deficient because of inadequate design, changes in loading requirements, damage due to corrosion or vandalism, ...etc. Carbon fiber reinforced polymer plates are attached to the bottom surface of beams while CFRP laminates are usually attached to the bottom surface or wrapped around the stem of RC rectangular and T-beams using epoxy adhesives. Laminates are preferable to plates because they are easier to handle, and they do not peel off as easily when compared to the more rigid CFRP plates. Examples of projects involving the use of CFRP plates and laminates to strengthen deficient concrete girders can be found in the state-of-the-art report published by ACI ¹.

Many experimental and analytical studies have been conducted to explore both the short- and long-term behavior of beams flexurally strengthened with CFRP laminates". These studies have focused on the effect of CFRP rehabilitation on the stiffness, strength, ductility, mode of failure, and reliability of reinforced concrete girders strengthened with CFRP laminates. Based

on the results of these studies, design models and methodologies have been proposed to identify the necessary number of laminates to achieve a target strength or stiffness^{4,9}. ACI committee 440 is currently developing design guidelines for external strengthening of concrete structures using fiber reinforced polymer systems, and a synthesis of the provisions of the Canadian Highway Bridge Design Code for fiber-reinforced structures has been recently published¹⁰.

One of the issues that have not been adequately resolved is the short-term tensile strength of CFRP composites for strengthening of concrete girders. Despite the fact that fiber reinforced polymer systems are no longer considered new materials established methods for estimating the design tensile strength are absent. ACI's state-of-the-art report acknowledges the issue; however, it falls short in recommending values or a specific method for estimating the design tensile strength of the product. This position is understood since products vary greatly by manufacturer, on the fiber type, fiber structure, and resin level. The state-of-the-art report suggests that loading conditions for the CFRP product be determined in advance and that the material characteristics corresponding to those conditions be obtained in consultation with the manufacturer. The work of Bakht et al.¹⁰ suggests the use of coupons for estimating the strength of FRP materials. While some researchers investigating uses of CFRP materials for strengthening applications have performed coupon tests to estimate the tensile strength of CFRP laminates (e.g. Ritchie et. al.²), there are some instances in the literature where laminate strength was assumed equal to the manufacturer reported fiber strength. This could be unconservative since the strength of a single fiber or dry strand is generally greater than the laminate strength. Nevertheless, an unconservative estimate of laminate strength is inconsequential if the modes of failure under study do not involve laminate rupture, but rather concrete and bond related failures.

Fibers are assembled together to form tows or yarns, which are then woven into a fabric that forms the laminate. Experimental testing and analyses¹¹⁻¹⁶ have shown that the strength of the final composite product (i.e. laminate), $\sigma_{lamin ate}$, is normally much lower than the strength of the fiber, σ_{fiber} , in some cases, as low as 40-50%. Several researchers¹¹⁻¹⁶ have investigated the relationship between σ_{fiber} and $\sigma_{lamin ate}$, and presented techniques for estimating laminate strength from fiber characteristics. However, these methods have yet to be adopted by structural engineers designing structures strengthened with CFRP laminates.

This paper investigates the short-term tensile strength of CFRP laminates used for strengthening concrete girders. The Weibull theory is used to establish a relationship between the fiber tensile strength and the tensile strength of CFRP laminates attached to a concrete girder. Such a relationship facilitates the design process and enables structural engineers to estimate laminate strength from fiber properties published by the manufacturer. While coupon and component tests are valid means for estimating the short-term tensile strength of CFRP sheets, they are not practical and, as will be illustrated in this paper, composite strength is affected by the coupon size. To verify the theory presented in the paper, the short-term tensile strength of CFRP sheets calculated using the proposed theory is compared to published experimental results of concrete T-beams strengthened with a varying amount of CFRP laminates. Good agreement is found between theoretical calculations and test results.

WEIBULL THEORY FOR COMPOSITE MATERIALS

The tensile strength of composite materials is assumed to follow the Weibull Theory. This assumption is well established in the literature^{12,13,17} and has been verified experimentally through tests of composite specimens with different size and stress distribution^{11,18,19}, especially for

unidirectional and $0^\circ/90^\circ$ laminates¹⁹. The basic concepts of the Weibull theory can be found in many textbooks (e.g. Batdorf¹⁷) and are summarized below for completeness.

If the average number of flaws per unit length of a fiber of a Weibull material is n , and the length a fiber is L , the expected number of flaws in the entire length, Q , is nL . Weibull theory expresses the number of flaws per unit length, n , in terms of the applied stress, σ , a shape parameter, m , and a scale parameter, σ_0 :

$$n(\sigma) = \left(\frac{\sigma}{\sigma_0} \right)^m \quad (1)$$

which leads to the following expression for the expected number of flaws for a fiber of a Weibull material of length L subjected to a strength less than σ .

$$Q = L \left(\frac{\sigma}{\sigma_0} \right)^m \quad (2)$$

To study the effect of the fiber on the failure strength of a Weibull material, the expected number of flaws, Q , has to be investigated. Failure takes place if there is a probability that one complete flaw exists; i.e. $Q = 1$. By setting $Q = 1$ in Eq. 2, the following expression is obtained for the expected failure stress:

$$\sigma_f = \sigma_0 L^{-1/m} \quad (3)$$

Figure 1 shows the effect of the length of the fiber on the expected failure stress of a Weibull material. It is clear that the strength of a fiber decreases as its length increases.

To generalize the theory, an infinitesimal fiber length, ΔL_j , is considered. The probability that the segment contains a flaw, which is equal to the probability of failure of the segment, is

$$(\Delta P_f)_j = n\Delta L_j \quad (4)$$

The probability of failure of an entire fiber of length L (comprised of N segments) is

therefore

$$P_f = 1 - \prod_{j=1}^N [1 - (\Delta P_f)_j] \quad (5)$$

For infinitesimal segment lengths ΔL_j , the probabilities of failure $(\Delta P_f)_j = n\Delta L_j$ are also infinitesimal, and hence the probability of failure of an entire fiber can be approximated as

$$P_f = 1 - \prod_{j=1}^N \exp[-(\Delta P_f)_j] = 1 - \exp\left[-\sum_{j=1}^N (\Delta P_f)_j\right] = 1 - \exp[-nL] \quad (6)$$

Making use of Eq.1, Eq. 6 can be expressed in the following alternatively form.

$$P_f = 1 - \exp\left[-\int_L (\sigma / \sigma_0)^m dL\right] \quad (7)$$

Equation 6 expresses the probability of failure, P_f , of a single fiber of a Weibull material in terms of its length, L , and the applied tensile stress, σ . It is useful to have a general form for the probability of failure expressed in terms of the volume instead of the length. This can be done by modifying Eq. 7 to read as follows.

$$P_f = 1 - \exp \left\{ - \int_v \left(\frac{\sigma}{\sigma_0} \right)^m dV \right\} \quad (8)$$

The relationships in Eq. 7 and Eq. 8 are usually referred to as the Weibull cumulative distribution functions. The shape and scale parameters in these equations are determined by calibration to test results ' and are related to the mean, and coefficient of variation, COV, through the following expressions.

$$\mu_0 = \sigma_0 \Gamma \left[\frac{1+m}{m} \right] = \sigma_0 \quad (9)$$

$$COV = \sqrt{\frac{\Gamma \left[\frac{2+m}{m} \right]}{\Gamma^2 \left[\frac{1+m}{m} \right]} - 1} \approx \frac{1.2}{m} \quad (10)$$

where $\Gamma[]$ is the gamma function. The approximations in Eqs. 9 and 10 have been made by several researchers including Batdorf¹⁷ and yield good results for the practical range of application.

Harlow and Phoenix¹² provided an "exact" formulation based on the chain-of-bundles model for the strength of *composite materials* comprised of many fibers. In this model, it is assumed that the composite material is formed of a chain of bundles in which each bundle consists of a number of fibers. Each of the fibers is assumed to have a Weibull distribution for the tensile strength; i.e. a Weibull material. Failure occurs when the weakest link of the entire formation reaches its load carrying capacity. The formulation of the problem provides a relationship between the failure of, the composite material and the size of the specimen. The work of Harlow

and Phoenix is laborious and is limited to two-dimensional applications. This led to several approximations of the exact behavior¹³⁻¹⁷. The following section summarizes the approximate method adopted in this research.

APPLICATION OF WEIBULL'S THEORY TO CFRP LAMINATES USED TO STRENGTHEN RC AND PC BEAMS

The tensile strength of CFRP laminates used to strengthen concrete girders can be estimated assuming that the fibers follow the Weibull theory. This goal will be achieved in two steps. The first -step deals with the size effect aspect of the behavior. After establishing a relationship between the strength of an individual fiber and a uniformly stressed laminate, a second treatment is needed to account for stress gradients.

Step.I: Size Effect

The size effect is accounted for following the approximate theory reported by Batdorf and Ghaffarian¹³. It is assumed that the number of flaws, Q_1 in a composite product that is uniformly-stressed and uniaxially-reinforced by a group of Weibull material fibers is

$$Q_i = NL \left(\frac{\sigma}{\sigma_0} \right)^{im} \prod_{k=1}^{i-1} c_k^m n_k \lambda_k \quad (11)$$

in which N is the number of fibers in the final product, L is the length of each fiber. The product of NL represents the entire volume of fibers in the composite; i.e. this formulation accounts for the volume or size effect. σ is the uniform stress acting on the composite product, n_k is the number of fibers immediately adjacent to a ruptured fiber that are affected by its

failure, λ_k is the effective length of the overloaded region affected by the rupture, c_k is the stress concentration factor in that region, σ_0 and m are the scale and shape parameters of the Weibull distribution representing the single fiber, and finally i is the number of adjacent fibers that are ruptured at the time of failure of the composite product. In the case of $i=1$, it is said that a singlet has formed. The formation of a singlet causes stresses in the adjacent fibers to increase due to stress concentrations. When an adjacent fiber ruptures, i increases to two and the condition is that of a doublet. As the stress increases, triplets and quadruplets ... etc. form. Once Q_i reaches unity; i.e. it is probable that a complete flaw exists in the product, and hence failure is eminent. Solution of Eq. 11 leads to the following relationship between the failure stress, $\sigma_{uniform}$, of a uniformly stressed laminate and that of the scale parameter, σ_0 , of a single fiber

$$\frac{\sigma_{uniform}}{\sigma_0} = \left[NL \prod_{k=1}^{i-1} c_k^m n_k \lambda_k \right]^{-1/im} \quad (12)$$

The value of m and σ_0 in the previous equation can be estimated using Eqs. 9 and 10. When applied to $0^\circ/90^\circ$ laminates, the total fiber length NL in Eq. 12 pertains to fibers aligned in the direction of the beam axis only. Transverse fibers do not participate significantly in flexural strengthening applications, and their contribute to the size effect will be negligible.

While N and L are physical quantities that can be easily estimated, n_k , λ_k , c_k are harder to quantify. Batdorf and Ghaffarian¹³ report that measured values for λ_k are around 0.1 mm. The number of adjacent fibers affected by a rupture at any stage, n_k , is taken between 2 and 15. The stress concentration factor, c_k , can be dealt with as a random variable¹² or a simplified form can be used as reported by Batdorf¹⁷.

$$c_k = 1 + 0.5k \quad (13)$$

The size effect expressed by Eq. 12 is illustrated in Fig. 2. The plot makes use of Eq. 13 and assumes that $\lambda_k = 0.1$ mm and $n_k = 8$ for all values of k . It should be noted that the failure surface (upper bound) of all possible i -plets defines whether failure is due to a singlet, doublet, etc. For example at $\ln(NL/\lambda) = 10$, singlets first form and as the stress increases doublets form. The material cannot resist stresses beyond the doublet level (failure surface bound) since it is clear from the figure that at this level triplets and beyond provide less resistance. The failure surface obtained from this approximate method is in good agreement with the more exact failure surface based on the theory of Harlow and Phoenix¹².

Step 11: Stress Gradient Effect

The previous derivation assumes that the composite is uniformly stressed. In many cases the stress distribution in the laminate is not uniform and another treatment of $\sigma_{uniform}$ needed to adjust the results derived in the previous section. For the case of a composite laminate subjected to a stress gradient (such as that attached to the web of a beam), the probability of failure can be expressed in integral form as follows

$$P_f^{beam} = 1 - \exp \left\{ - \int_v \left(\frac{\sigma}{\sigma_0} \right)^{im} dV \right\}$$

The difference between Eq. 14 and Eq. 8 is that m is replaced with im , where i is the number of i -plets expected at failure. This modification follows directly from the work of Batdorf and

Ghaffarian¹³ and is necessary to account for the decrease in coefficient of variation of the laminate strength that has been observed experimentally¹¹.

For the case of a composite laminate subjected to a uniform stress, Eq. 14 yields

$$P_f^{uniform} = 1 - \exp \left\{ - \left(\frac{\sigma_{uniform}}{\sigma_0} \right)^{im} V_{uniform} \right\} \quad (15)$$

where $V_{uniform}$ the volume of the uniformly stressed composite, and $\sigma_{uniform}$ is the uniform stress it is subjected to.

The relationship between the failure strength of a uniformly stressed composite and that of a nonuniformly stressed composite is established by equating the expressions for the probability of failure; i.e. $P_f^{beam} = p_f^{uniform}$. The following section establishes the value of failure stress for the constant moment case. Appendix A gives the strength ratio $\sigma_{beam} / \sigma_{uniform}$ for several other common configurations.

Constant Moment Case

The derived expressions are for CFRP laminates that are wrapped around the web of a concrete girder. The wrap-around detail is considered in this derivation because it has been shown to provide better performance than attaching the CFRP sheets to the bottom of the girder. Wrapping the girder web with CFRP reduces the possibility of concrete delamination and bond failure between the concrete and CFRP⁸. In deriving the following expressions it was assumed that the stress at the top laminate fiber is equal to zero as shown in Fig. 3. This assumption is justified because the top of the laminate is close to the neutral axis. For the cases where CFRP

sheets are only attached to the bottom of the girder (e.g. slab bridges), a value of zero can be used for V_{web} below. The coordinate system used in deriving the following expressions is shown in Figs. 3 and 4.

The stress state is different in the bottom part (having volume V_{bottom}) of the CFRP sheet than it is in the webs (having volume V_{web}). Hence, the integral portion of Eq. 14 will be evaluated separately.

Bottom Contribution:

A uniform stress distribution is assumed for the bottom part, since no stress variations exist in this case. The integral in Eq. 14 is determined as

$$\int_{V_{bottom}} \left(\frac{\sigma}{\sigma_0} \right)^{im} dV = \int_{x=0}^{x=L} \int_{y=0}^{y=t} \int_{z=-b/2}^{z=b/2} \left(\frac{\sigma}{\sigma_0} \right)^{im} dz dy dx = btL \left(\frac{\sigma}{\sigma_0} \right)^{im} = V_{bottom} \left(\frac{\sigma}{\sigma_0} \right)^{im} \quad (16)$$

Web Contribution:

A linear stress distribution is assumed for the web parts:

$$\sigma(x, y, z) = -\frac{y}{h_{CFRP}} \sigma \quad (17)$$

Accordingly the integral in Eq. 14 is determined as

$$\int_{V_{web}} \left(\frac{\sigma}{\sigma_0} \right)^{im} dV = \int_{x=0}^{x=L} \int_{y=0}^{y=-h_{CFRP}} \int_{z=0}^{z=t} \left(\frac{y}{h_{CFRP}} \frac{\sigma}{\sigma_0} \right)^{im} dz dy dx = \frac{h_{CFRP} t L}{(im+1)} \left(\frac{\sigma}{\sigma_0} \right)^{im} = \frac{V_{web}}{(im+1)} \left(\frac{\sigma}{\sigma_0} \right)^{im} \quad (18)$$

Total (Web and Bottom) Contribution:

Adding both integrals

$$\int_V \left(\frac{\sigma}{\sigma_0} \right)^{im} dV = V_{bottom} \left(\frac{\sigma}{\sigma_0} \right)^{im} + 2 \frac{V_{web}}{im+1} \left(\frac{\sigma}{\sigma_0} \right)^{im} = \left(V_{bottom} + 2 \frac{V_{web}}{im+1} \right) \left(\frac{\sigma}{\sigma_0} \right)^{im} \quad (19)$$

In the previous expressions, V_{bottom} is the volume of the bottom part of the wrapped laminate, and V_{web} is the volume of the laminate attached to each side of the web.

Using Eq. 14, the probability of failure can be expressed in terms of the volumes of the CFRP parts.

$$P_f^{beam} = 1 - \exp \left\{ - \left(\frac{\sigma_{beam}}{\sigma_0} \right)^{im} \left[V_{bottom} + 2 \frac{V_{web}}{im+1} \right] \right\} \quad (20)$$

The ratio between the failure stress of the beam laminate, σ_{beam} , and that of a uniformly stressed laminate, $\sigma_{uniform}$, can be obtained by setting $P_f^{beam} = P_f^{uniform}$ which will lead to

$$V_{uniform} \left(\frac{\sigma_{uniform}}{\sigma_0} \right)^{im} = \left(V_{bottom} + 2 \frac{V_{web}}{im+1} \right) \left(\frac{\sigma_{beam}}{\sigma_0} \right)^{im} \quad (21)$$

This results in the following expression relating the failure stress of a uniformly stressed composite and that of a composite sheet wrapped around the web of a beam subjected to constant bending moment.

$$\frac{\sigma_{beam}}{\sigma_{uniform}} = \left(\frac{(im+1)V_{uniform}}{(im+1)V_{bottom} + 2V_{bottom} + 2V_{web}} \right)^{1/im} \quad (22)$$

In Eqs. 20 and 21, both uniformly and nonuniformly stressed laminates must be of similar size to develop the same type of *i*-plet failure.

VERIFICATION OF THEORY

The experimental work reported by Shahawy and Beitelman⁸ is used to verify the applicability of the theory to strengthening schemes involving the use of CFRP sheets. The tested beams serve the purpose of the verification study because the CFRP laminates ruptured in the high flexure region. Many of the experimental results reported in the literature cannot be used for verification because other modes of failure were observed (concrete crushing, delamination of CFRP, ...etc.). Figures 5 and 6 show the dimensions of the tested beams. The properties of the CFRP fibers of which the laminates were woven are given in Table 1. Table 2 gives the reinforcing steel and concrete properties for each of the studied beams.

Short-term Tensile Stress

The first step in the process is to find σ_{uniform} based on fiber strength provided by the manufacturer, σ_{fiber} . At this stage, it will be first assumed that the total volume (803 mm x 5791 mm x t_{CFRP} [31.6in x 228in x t_{CFRP}]) of the CFRP laminates is uniformly stressed. The number of longitudinal yarns in a single layer of CFRP laminate is equal to (14+3.6+14) in x (6) yarns/in = 190 with 12,000 fibers in each yarn; i.e. $N = 2275200$ fibers. The data provided by the manufacturer (Table 1) does not give the COV of CFRP fibers. It was therefore assumed that COV is 6.86% which corresponds to values of $m = 18$ and $\sigma_0 = 546$ ksi according to Eqs. 9 and 10. The choice of $m = 18$ is based on a review of the experimental results reported by several researchers^{11,18,19}, which showed that for FRP fibers m ranges between 10 and 29. The length of

each fiber is $L = 5791$ mm [228 in]. Using $n_k = 8$, $\lambda_k = 0.1$ mm, and c_k as suggested in Eq. 13, it was found that a triplet failure ($i = 3$) will take place for W-1L5, and that $\sigma_{uniform}/\sigma_0$ is equal to 0.5435 according to Eq. 12.

Since failure happened due to the formation of a triplet flaw (i.e. $i = 3$), then $im = 3 \times 18 = 54$ in the following stress gradient calculations. The effect of the stress gradient in the web portions is accounted for in the second step, which is performed by substituting the cross-sectional properties into Eq. A.4. The result is $\sigma_{beam}/\sigma_{uniform}$ equal to 1.059. Combining both effects leads to a σ_{beam}/σ_0 ratio of 0.576; i.e. $\sigma_{beam} = 2.17$ Gpa [314.4 ksi]. It is clear that the size effect has a much greater impact on the short-term strength of the composite sheet than the stress gradient effect has. The same procedure was repeated for the other specimens using the appropriate number of fibers for each case (e.g. $N = 6825600$ fibers for W-3L5). The failure stress predicted by the theory is used as input for a fiber section analyses of the test beams.

Fiber-Section Analysis

The verification study is conducted by performing fiber-section analyses of the specimen cross-sections. The analyses are conducted using a computer program developed for this purpose. As shown in Fig. 7, fiber section analyses of a composite cross section entails discretization of the section into many layers (fibers) for which the constitutive models are based on uniaxial stress-strain relationships. Each region represents a fiber of material running longitudinally along the member and can be assigned one of several constitutive models representing concrete, CFRP, or reinforcing steel. The main assumptions employed in the fiber section method are as follows:

- Plane sections are considered to remain plane after bending. It is generally accepted that this assumption is reasonably good even well into the inelastic range. Measurements of strains along the height show that this assumption is accurate for beams with either partial or full wrapping^{8,20}.
- Shear stresses are not accounted for. The fiber section method, as presented in this paper, is therefore limited to long thin members whose behavior is dominated by flexure.

The general solution procedure is organized around calculating the moment-curvature response for a fixed value of axial load, P , where, $P=0$ for the case of pure flexure. The moment curvature response is obtained by incrementally increasing the curvature and solving for the corresponding value of moment. The location of the neutral axis and the fiber strains are a function of the curvature, ϕ , and strain at the extreme top fiber, ϵ_{top} . Based on the "plane sections remain plane" assumption, the fiber strains are equal to the product of the curvature times the orthogonal distance from the centroid of each fiber to the neutral axis. If needed, fiber strains for the concrete deck and the CFRP laminate are adjusted to account for any different initial conditions at the time of their contribution as can be seen in Fig. 7. The fiber stresses are calculated from the fiber strains using the constitutive relations shown in Fig. 6. The axial force in the cross-section (P) is calculated by summing up the product of the fiber stresses and fiber areas. For given values of curvature, the top fiber strain is solved for by iteration until the specified value of P is reached. Resulting from this process is a set of unique values of moment, M , and curvature, ϕ . The moment-curvature calculations are stopped when a prespecified number of curvature increments are applied. Details of the method can be found elsewhere²¹.

Comparison of Flexural Capacities

Table 2 summarizes the results of the verification study. The designation of the beams describes the number of CFRP layers used and concrete strength; e.g. W-3L5 is strengthened with 3 layers and has a nominal concrete compressive strength of $f'_c=5$ ksi. It can be seen from Table 2 that the flexural capacities (M_{max}) obtained from the analyses and the values observed from the tests are in good agreement (average difference of -3.0%). The maximum difference is -6.8%. The flexural capacity as predicted by the analysis based on the suggested short-term tensile strength is on the conservative side for all beams except Beam W-4L5 where the analysis predicts a slightly higher M_{max} ($\Delta M_{max} / M_{max} = +2.6\%$).

While this verification study is rather limited, it does suggest that the proposed method can be used to reasonably estimate the short-term tensile strength of CFRP laminates. Nevertheless, further verification of the method should be sought through comparisons to additional tests of beams with different size and load configurations.

DESIGN IMPLICATIONS

The work described in this paper has important implications regarding the applicability of coupon test results. Coupon tests are typically conducted using relatively small specimens, and may therefore lead to unconservative estimates of strength if the size effect is not properly considered. For coupons to be representative of the final structure, they should be large enough to develop the same type of multi-plet that is expected in the actual-size structure. While such a size may be relatively small, the size of the specimen should be studied before the results can be

considered reliable for design purposes. The methodology described in this paper and represented by Eq. 12 and Fig. 2 can be used for this purpose.

An alternative approach that is more suited for implementation in design guidelines is to develop design charts from which engineers can extract the short-term strength of CFRP laminates. Figure 9 is a plot of the relationship between the total length of fibers in a composite, NL , and the strength ratio, σ_f / σ_0 calculated according to Eq. 12. The plot is obtained using the same parameters used to compute Fig. 2, i.e. $m = 18$, c_k from Eq. 13, $\lambda_k = 0.1$ mm., and n_k 8 for all values of k . These parameters are chosen following Batdorf and Ghaffarian¹³ and Batdorf¹⁷ and were found to give reasonable results in the verification study described in the previous section.

The input to the developed design chart is the total length of all the fibers in the composite structure, NL , and the output is the ratio of the short-term tensile strength, σ_f , to the scale factor, σ_0 , which can be taken equal to σ_{fiber} for all practical purposes following the approximation in Eq. 9. To illustrate the method, the dimensions of verification beam W-1L5 will be used. The total length of fibers can be estimated as 5791 (mm) \times 190 (yarn) \times $12,000$ (fibers/yarn) = 13.2×10^9 mm. The corresponding short-term tensile strength is $\sigma_{f,max} = 0.5435 \times 3.65 = 1.984$ GPa [287.7 ksi] and a triplet failure type is expected ($i = 3$ from chart). This stress still needs to be adjusted to account for the stress gradient effect using $i = 3$ (previously calculated to be 1.059). The stress gradient effect is typically less than 10% and can be conservatively ignored when estimating the short-term tensile strength of CFRP laminates. The developed chart is suitable for general-purpose carbon fiber reinforced polymer laminates. Similar charts can be developed for other types of CFRP laminates.

The chart in Fig. 9 is developed assuming that the reported fiber strength is for fibers with a gauge length of 25.4mm [1in]. This gauge length is frequently used in fiber and dry strand tests²². In cases where the manufacturer reports a different gauge length, the reported stress can be adjusted to the 25.4mm [1in] gauge length strength using the following factor, which stems from Eq. 7.

$$\text{Gauge Length Factor} = \frac{\sigma_{fiber1}}{\sigma_{fiber2}} = \left(\frac{L_1}{L_2} \right)^{-1/m} \quad (23)$$

The tensile strength computed from the chart represents the short-term strength. The design tensile strength should account for additional reductions due to environmental exposure conditions (temperature, humidity, and chemical exposure) as well as load characteristics (long term and repeated).

SUMMARY AND CONCLUSIONS

The short-term tensile strength of CFRP laminates used for strengthening concrete girders can be estimated by applying the Weibull Theory. Two steps are needed to calculate the short-term tensile strength. The first step accounts for the size effect and predicts the tensile strength of a uniformly stressed volume that shares the size of the CFRP used in the real structure. The second step accounts for the effect of stress gradients. Expressions that account for the stress gradient effect in several common load configurations are derived and presented. Analytical results calculated using the developed theory are compared to published test results of reinforced concrete T-beams strengthened with CFRP laminates. Good agreement is found between theoretical calculations and test results. The work described in this paper suggests that coupon tests may lead to unconservative estimates of strength if the size effect is not properly

considered. Based on the work presented in this paper, a design tool is provided in the form of a chart which can be used to estimate the effect of size on the short-term tensile strength of CFRP laminates.

ACKNOWLEDGEMENTS

The authors gratefully acknowledge the financial support provided in part by the Florida Department of Transportation (Contract # BC-190) and the Department of Civil and Environmental Engineering at the University of Central Florida.

REFERENCES

1. ACI, *State-of-the-Art Report on Fiber Reinforced Plastic Reinforcement for Concrete Structures*, Report by ACI Committee 440, American Concrete Institute, Box 19150, Redford Station, Detroit, Michigan 48219, USA, 1996.
2. Ritchie, P.A., Thomas, D.A., Lu, L., and Connelly, G.M. "*External Reinforcement of Concrete Beams Using Fiber Reinforced Plastics*," *Structural Journal*, ACI, Vol. 88, No. 4, 1991, pp. 490-500.
3. Saadatmanesh, M.A., and Ehsani, M.R. "*RIC Beams Strengthened with GFRP plates 1: Experimental Study*," *Journal of Structural Engineering*, ASCE, Vol. 117, No. 10, 1991, pp. 3417-3433.
4. Jones, R., and Swamy, N. "*Strengthening of Reinforced Concrete T-beams by Epoxy Bonded Plate Technique*," *Proceedings of ACI Convention*, ACI, 1992.
5. Triantafillou, T.C. and Pelvris, N. "*Strengthening of RC Beams with Epoxy-bonded FibreComposite Materials*," *Materials and Structures*, Vol. 25, 1992, pp. 201-211.
6. Shahawy, M., and Beitelman T.E. "*Structural Applications of Advanced Composite Materials in Bridge Construction and Repair*," *Proceedings of the XIII ASCE Structures Congress*, ASCE, Reston, VA, 1995.
7. Arduini, M. and Nanni, A. "*Parametric Study of Beams with externally Bonded FRP Reinforcement*," *Structural Journal*, ACI, Vol. 94, No. 5, 1997, pp. 493-501.
8. Shahawy, M., and Beitelman T.E. "*Static and Fatigue Performance of RC Beams Strengthened with CFRP Laminates*," *Journal of Structural Engineering*, ASCE, Vol. 125, No. 6, 1999, pp. 613-621.

9. Saadatmanesh, H. and Malek, A. M. "*Design Guidelines for Flexural Strengthening of RC Beams with FRP Plates*," Journal of Composites for Construction, Vol. 2, No. 4, 1998, pp. 158-164.
10. Bakht, B., Al-Bazi, G., Banthia, N., Cheung, M., Erki, M., Faoro, M., Machida, A., Mufti, A., Neale, K., and Tadros, G. "Canadian Bridge Design Code Provisions for Fiber-Reinforced Structures," Journal of Composites for Construction, ASCE, Vol. 4, No. 1, 2000, pp. 3-15.
11. Bullock, R.E. "*Strength Ratios of Composite Materials in Flexure and in Tension*," Journal of Composite Materials, Vol. 8, 1974, pp. 200-206.
12. Harlow, D.G. and S.L. Phoenix. "*Probability Distributions for the Strength of Composite Materials H. A Convergent Sequence of Tight Bounds*," International Journal of Fracture, Sijthoff & Noordhoff International Publishers, Vol. 17, No. 6, 1981, pp. 601-630.
13. Batdorf, S.B. and R. Ghaffarian. "*Size Effect and Strength Variability of Unidirectional Composites*," International Journal of Fracture, Martinus Nijhoff Publishers, Vol. 26, 1984, pp. 113-123.
14. Duva, J.M., Aboudi, J, and Herakovich, C.T. "*A probabilistic Macromechanical Model for Damaged Composites*," Journal of Engineering Materials and Technology, ASME, Vol. 118, No. 4, 1996, pp. 548-553.
15. Mahadevan, S., Liu, X., and Xiao, Q. "*A Probabilistic Failure Model of Composite Laminates*," Journal of Reinforced Plastics and Composites, Technomic Publishing Co., Vol. 16, No. 11, 1997, pp. 1020-1038.

16. Yushanov, S.P., and Bogdanovich, A.E. *"Analytical Probabilistic Modeling of Initial Failure and Reliability of Laminated Composite Structures,"* International Journal of Solids and Structures, Pergamon, Vol. 35, No. 7-8, 1998, pp. 665-685.
17. Batdorf, S. B. *Concise Encyclopedia of Composite Materials*, Revised Edition, Edited by A. Kelly, Pergamon, MIT, Cambridge, MA, USA, 1994.
18. Kaminski, B.E. *"Effects of Specimen Geometry on the Strength of Composite Materials,"* Analysis of the Test Methods for High Modulus Fibers and Composites, ASTM, STP 521, 1973, pp. 181-191.
19. Lavoie, J. A. *Scaling Effects on Damage Development, Strength, and Stress-rupture Life on Laminated Composites in Tension*, Ph.D. Dissertation, Virginia Tech, Blacksburg, VA, USA, 1997.
20. Inoue, S., Nishibayashi, S., Kuroda, T., and Omata, F. *"Fatigue Strength and Deformation Characteristics of Reinforced Concrete Beams Strengthened with Carbon Fiber-Reinforced Plastic Plate,"* Transactions of the Japan Concrete Institute, Vol. 17, 1995, 149-156.
21. El-Tawil, S., Okeil, A.M., and Ogunc, C. *Static and Fatigue Behavior of RC Beams Strengthened with CFRP Laminates*. Research Report, Department of Civil and Environmental Engineering, University of Central Florida, Orlando, Florida, 1999.
22. McMahon, P.E. *"Graphite Fiber Tensile Property Evaluation,"* Analysis of the Test Methods for High Modulus Fibers and Composites, ASTM, STP 521, 1973, pp. 367-389.

LIST OF NOTATIONS

b	bottom width of beam cross section
c_k	stress concentration factor for adjacent fibers due to a k -plet
f'_c	concrete compressive strength
f_y	steel yield stress.
h_{CFRP}	height of CFRP laminate wrapping of web
M_{max}	flexural capacity of beam
ΔM_{max}	difference between flexural capacities obtained from analysis and tests
n	number of flaws per unit length of a CFRP fiber
n_k	number of adjacent fibers affect by the a fiber rupture due to a k -plet
N	total number of fibers in a CFRP laminate
P_f	probability of failure of a composite fiber
$P_f^{uniform}$	probability of failure of a uniformly stressed composite laminate
P_f^{beam}	probability of failure of a composite laminate wrapped around the stem of a beam
Q	expected number of flaws in a CFRP fiber

t	thickness of CFRP laminate.
V_{uniform}	volume of a uniformly stressed CFRP laminate
V_{beam}	volume of a CFRP laminate wrapped around the stem of a beam
V_{bottom}	volume of the CFRP laminate attached to the bottom part of a beam
V_{Web}	volume of the CFRP laminate attached to one side of the web of a
ϕ	beam curvature of cross section due to flexure
ϵ_{top}	strain at the extreme top fiber of the cross section
σ	stress in CFRP laminate.
σ_{fiber}	tensile strength of a single CFRP fiber (as reported by manufacturer)
σ_{laminate}	expected short-term tensile strength of a CFRP laminate
σ_{uniform}	expected short-term tensile strength of a uniformly stressed CFRP laminate
σ_{beam}	expected short-term tensile strength of a CFRP laminate wrapped around the stem of a beam
m, σ_0	shape and scale parameters of a Weibull distribution for strength of composite materials
$\Gamma[]$	gamma function

- μ_σ mean of the short-term tensile strength of a Weibull material
- COV coefficient of variation of the short-term tensile strength of a Weibull material
- λ_k effective length of the overloaded region affected by the rupture due to a k -plet

APPENDIX A. STRENGTH RATIO OF CFRP SHEETS IN FLEXURE AND TENSION:
STRESS GRADIENT EFFECT

In addition to the case of a beam under constant moment discussed in the main body of the paper, three other common load configurations are considered in investigating the stress gradient effect. The load configurations are uniformly distributed load, single concentrated load, and four point load configurations (see Fig. 10).

Case I: Concentrated load at mid-span

Following the procedure for accounting for stress gradients described in the main body of the paper, an expression can be obtained for the case of a beam subjected to a concentrated load acting at midspan. In this case the stress varies linearly in the longitudinal direction with a peak at midspan. This leads to the following expression for the stress in the bottom part of the CFRP sheet

$$\sigma(x, y, z) = \frac{2x}{L} \sigma \quad [A.1]$$

and similarly the next expression for the web parts:

$$\sigma(x, y, z) = -\frac{2x}{L} \frac{y}{h_{CFRP}} \sigma \quad [A.2]$$

These stress expressions lead to the following relationship between $\sigma_{uniform}$ and σ_{beam}

$$\frac{\sigma_{beam}}{\sigma_{uniform}} = \left(\frac{(im+1)^2 V_{uniform}}{(im+1)V_{bottom} + 2V_{web}} \right)^{1/im} \quad [A.3]$$

Case II: Four point loading (Constant Moment Region)

The integrals for both the web parts and the bottom part are evaluated in two steps since each part comprises of two regions; a constant moment region, and a linear moment region. The CFRP sheet volumes will be designated using a superscript for the part they represent; e.g. V_{web}^{linear} and $V_{web}^{constant}$. The following relationship is obtained:

$$\frac{\sigma_{beam}}{\sigma_{uniform}} = \left(\frac{(im+1)^2 V_{uniform}}{(im+1)^2 V_{bottom}^{constant} + (im+1)[V_{bottom}^{linear} + 2V_{web}^{constant}] + 2V_{web}^{linear}} \right)^{1/im} \quad [A.4]$$

Case III: Uniformly distributed load

A general closed-form solution for the integral is only possible in terms of the gamma function, $\Gamma[\]$. The evaluation of the integral leads to the following stress relationship

$$\frac{\sigma_{beam}}{\sigma_{uniform}} = \left(\frac{2(im+1)^2 V_{uniform}}{\pi^{1/2} \frac{\Gamma[2+im]}{\Gamma[3/2+im]} \{(im+1)V_{bottom} + 2V_{web}\}} \right)^{1/im} \quad [A.5]$$

LIST OF TABLES:

Table 1: Properties of CFRP Laminates (Provided by manufacturer) 31

Table 2: Comparison of Failure Moments.....32

LIST OF FIGURES:

FIGURE 1: Effect of fiber length on failure stress (Weibull size effect) 33

FIGURE 2: Effect of composite size on damage sequence based on approximate method. ($n_k=8$, $\lambda_k=0.1$ mm, $c_k=1+0.5 k$) 34

FIGURE 3: Normal stress distribution in CFRP sheets due to flexure (a-wrap-around detail, b-normal stress distribution on bottom and web parts)..... 35

FIGURE 4: Coordinate system for integration purposes (Case of constant moment) 36

FIGURE 5: Loading setup for FDOT girders (dimensions in inches)37

FIGURE 6: Cross-section details (dimensions in inches) 38

FIGURE 7: Schematic of the fiber section technique used for verification (Prestressed girder with composite deck and CFRP sheets) 39

FIGURE 8: Constitutive relationships used for fiber section analysis (a-concrete, b- steel, CFRP). 40

FIGURE 9: Proposed chart for predicting the short-term tensile strength of uniformly stressed CFRP sheets.....41

FIGURE 10: Loading configurations considered in Appendix A (a-concentrated load, b-four-point loading, c-uniform load) 42

Table 1: Properties of CFRP Laminates (Provided by manufacturer)

Property	Value
Fiber Tensile Strength (σ_{fiber})	3.65 GPa [530 ksi]
Modulus of Elasticity (Tension)	231 GPa [33,500 ksi]
Filament Diameter	7 μm
Filaments/yarn	12,000
Yarn density	0.23/mm [6/inch]
Ultimate Elongation	1.4%

Table 2: Comparison of Failure Moments

Specimen	Material Strength, MPa [ksi]			Flexural Capacity (M_{max})		
	Yield Stress (f_y)	Concrete Strength (f_c')	CFRP Strength (σ_f)	Experiment KN-m[kip-in]	Analysis kN-m [kip-in]	Difference* (%)
W-1L5		35.9 [5.2]	2200[314.4]	211.4 [1871]	205.0 [1813]	-3.1
W-2L5-A		37.2 [5.4]	2140[310.4]	259.5 [2300]	243.5 [2155]	-6.3
W-2L5-B	441[64]	35.1 [5.11]	2140[310.4]	259.9 [2300]	242.2 [2143]	-6.8
W-3L5		35.1 [5.11]	2120[308.11]	282.5 [2500]	278.5 [2464]	-1.4
W-4L5		35.1 [5.11]	2110[306.4]	305.1 [2700]	313.1 [2770]	+2.6
					Average	-3.0

* (+) indicates unconservative prediction, (-) indicates conservative prediction

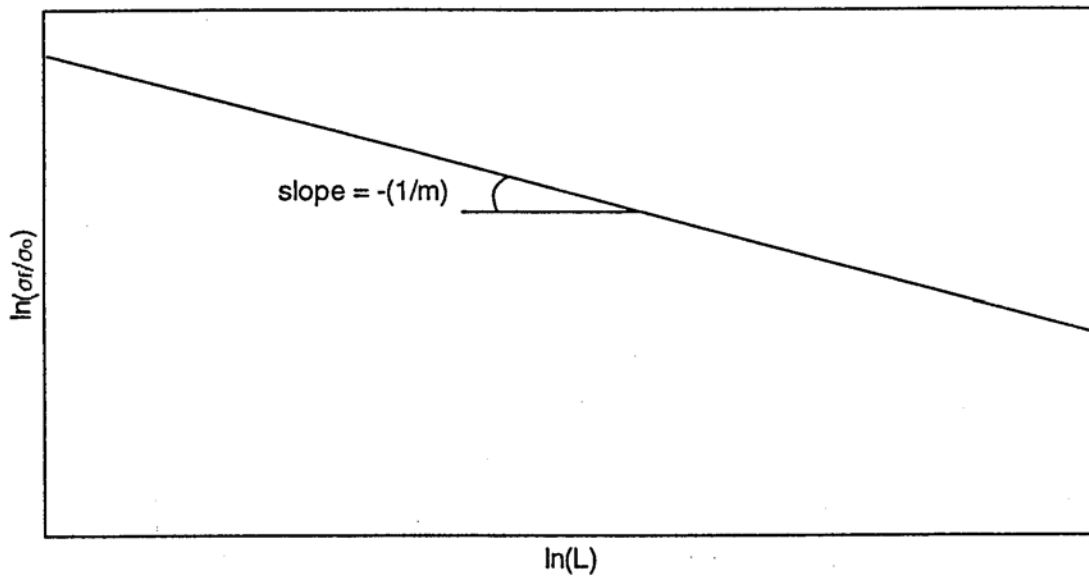


FIGURE 1: Effect of fiber length on failure stress (Weibull size effect)

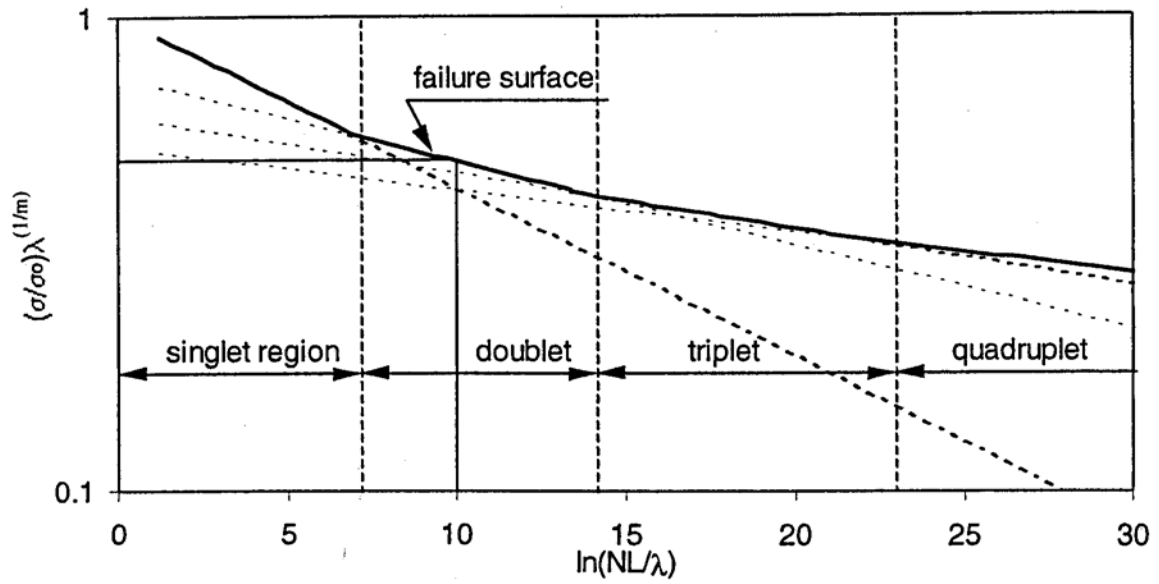


FIGURE 2: Effect of composite size on damage sequence based on approximate method. ($n_k=8$, $\sim k=0.1$ mm, $c_k=1+0.5 k$)

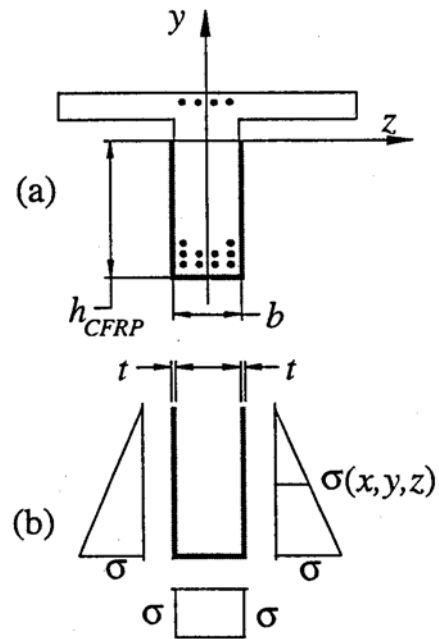


FIGURE 3: Normal stress distribution in CFRP sheets due to flexure (awrap-around detail, b-normal stress distribution on bottom and web parts).

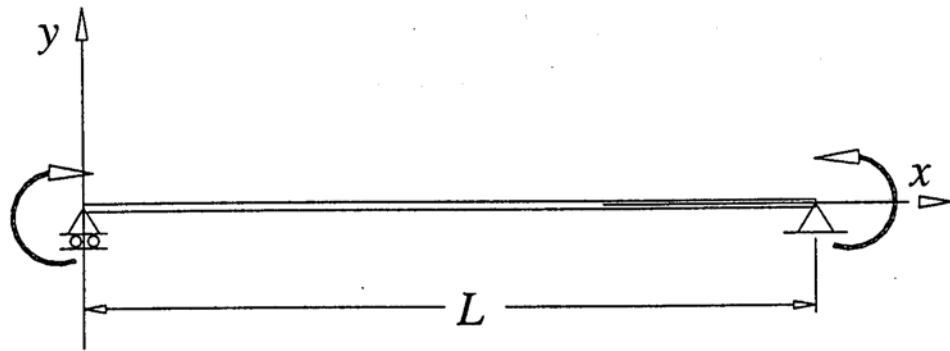


FIGURE 4: Coordinate system for integration purposes (Case of constant moment)

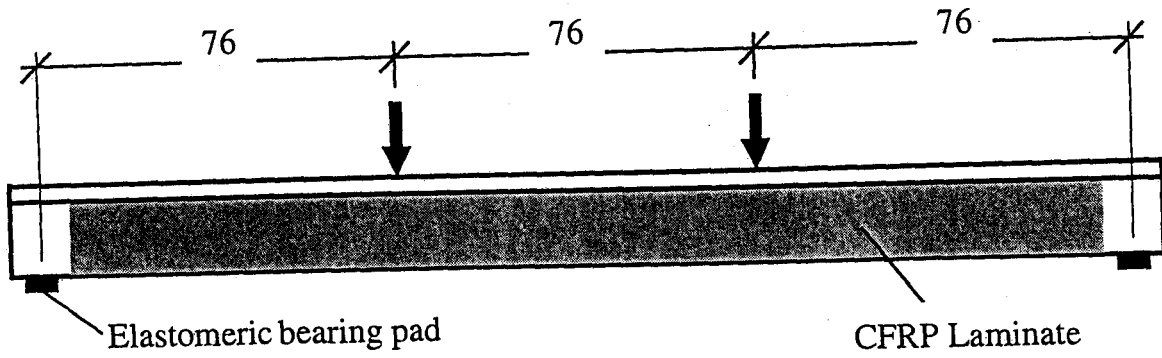


FIGURE 5: Loading setup for FDOT girders (dimensions in inches)

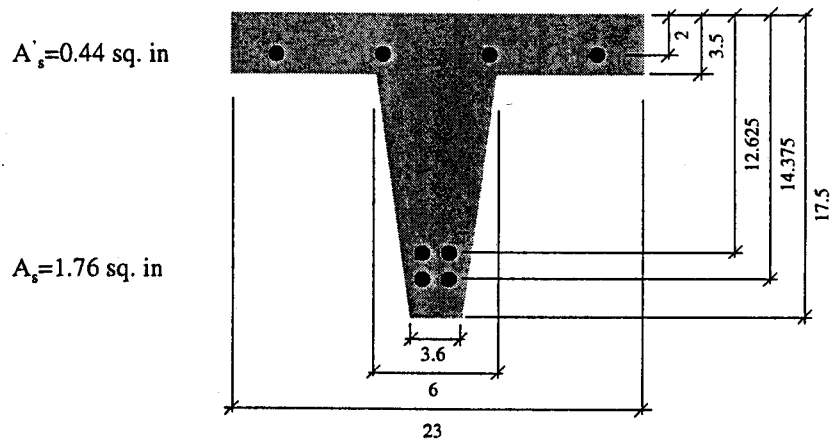


FIGURE 6: Cross-section details (dimensions in inches)

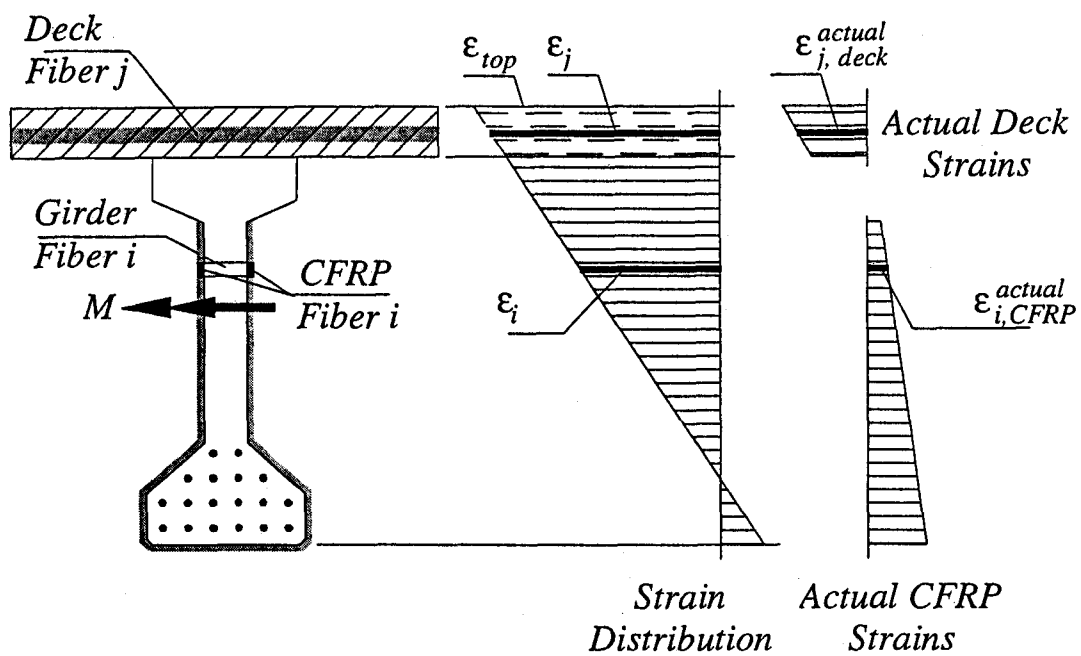


FIGURE 7: Schematic of the fiber section technique used for verification
(Prestressed girder with composite deck and CFRP sheets)

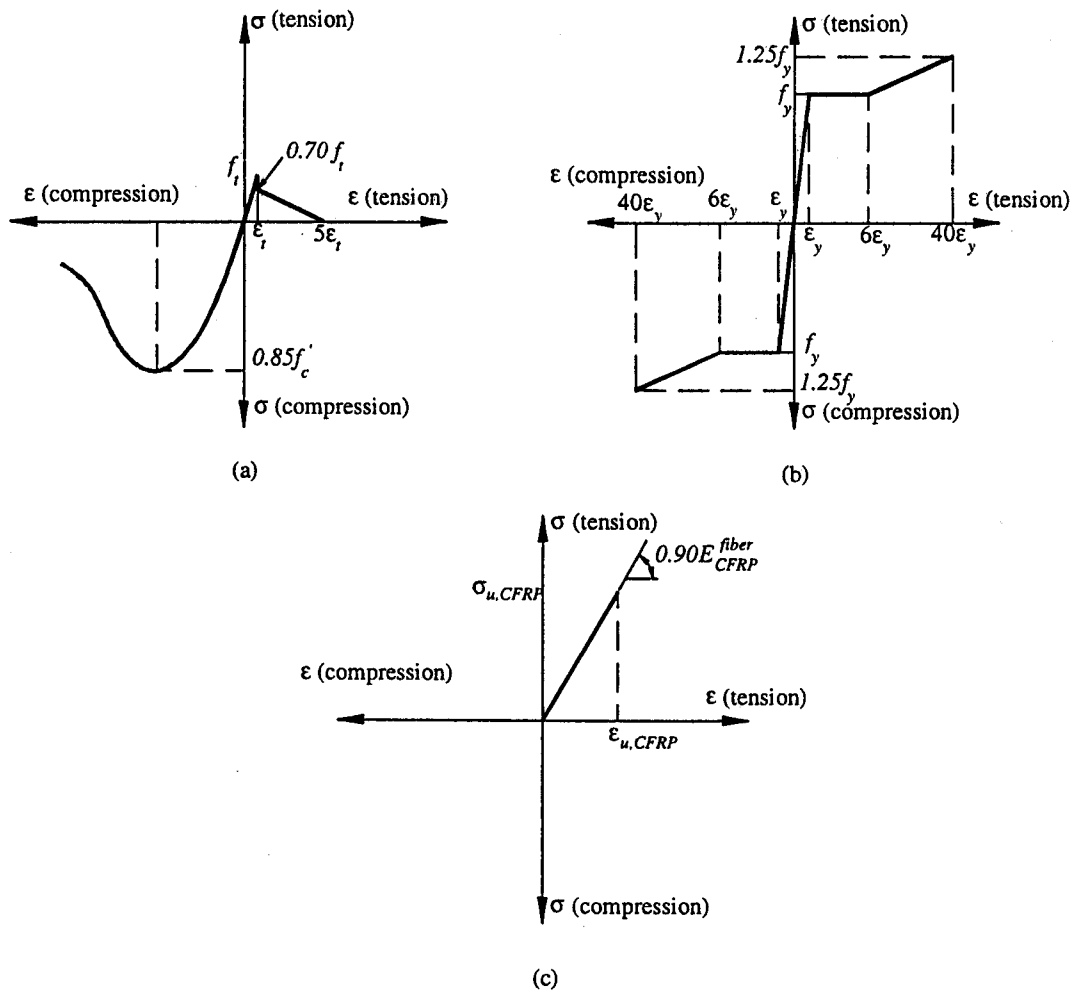


FIGURE 8: Constitutive relationships used for fiber section analysis (a-concrete, b- steel, c-CFRP).

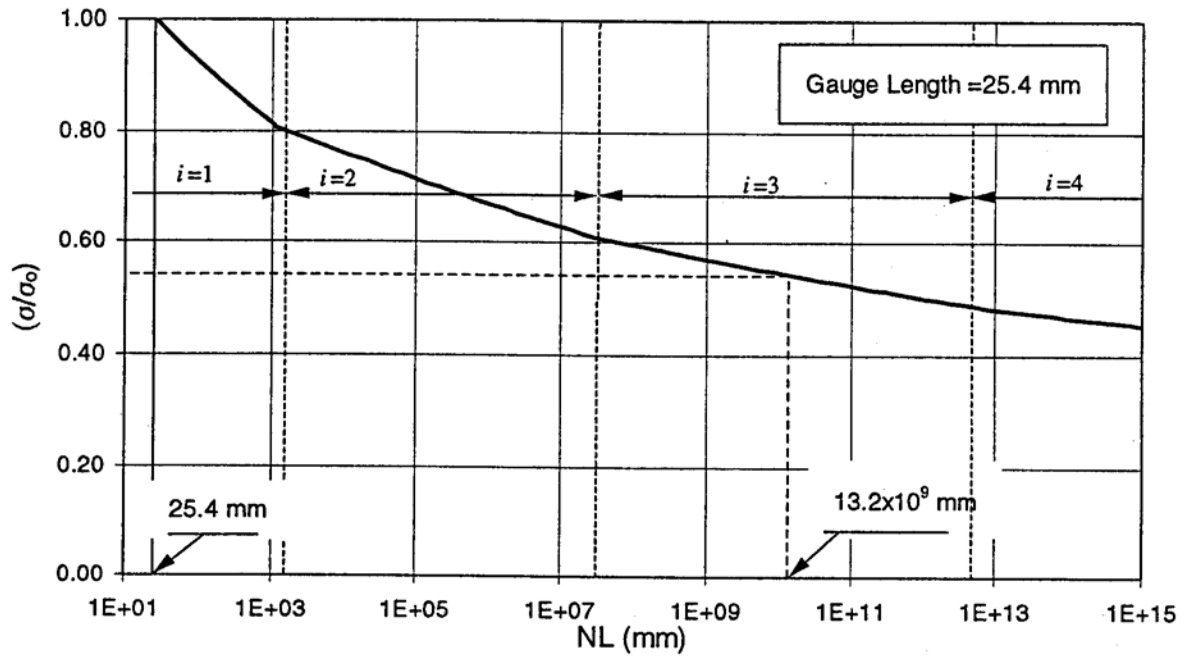


FIGURE 9: Proposed chart for predicting the short-term tensile strength of uniformly stressed CFRP sheets.

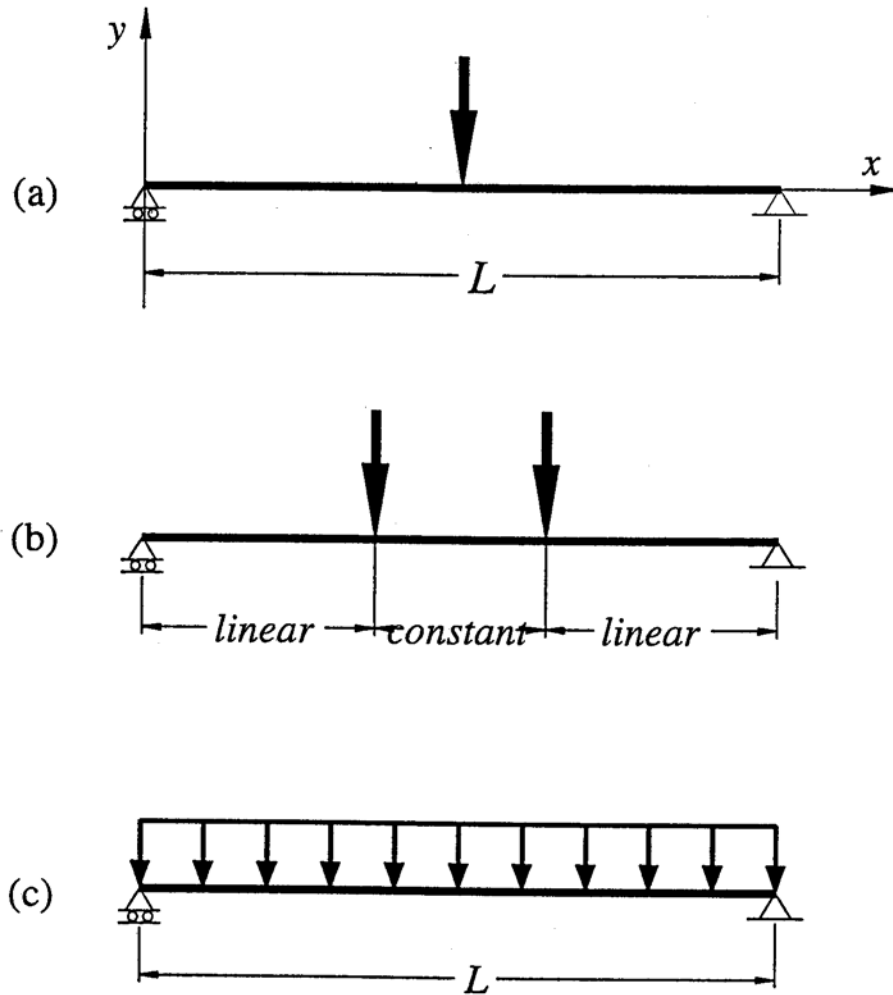


FIGURE 10: Loading configurations considered in Appendix A (a concentrated load, b-four-point loading, c-uniform load)

BIOGRAPHIES

Ayman M. Okeil is an assistant professor in the Dept. of Structural Engineering at Alexandria University, Alexandria, Egypt. Currently, he is visiting the Dept. of Civil and Environmental Engineering at the University of Central Florida, Orlando, Florida. He obtained his BS and MS degrees from Alexandria University, and his PhD degree from North Carolina State University. His research interests include nonlinear analysis and design of concrete structures, bridge engineering, structural reliability, seismic design.

Sherif EI-Tawil is an assistant professor in the Dept. of Civil and Environmental Engineering at the University of Central Florida, Orlando, FL, USA. His research focuses on the seismic behavior and design of composite steel-concrete and FRP reinforced structures. He is a member of ACI committee 335.

Mohsen Shahawy is chief structural analyst in the Structural Research Center, Florida Department of Transportation. He has been involved in numerous studies on the behavior and performance FRP reinforced structures and is a member of several ACI committees including ACI 440.